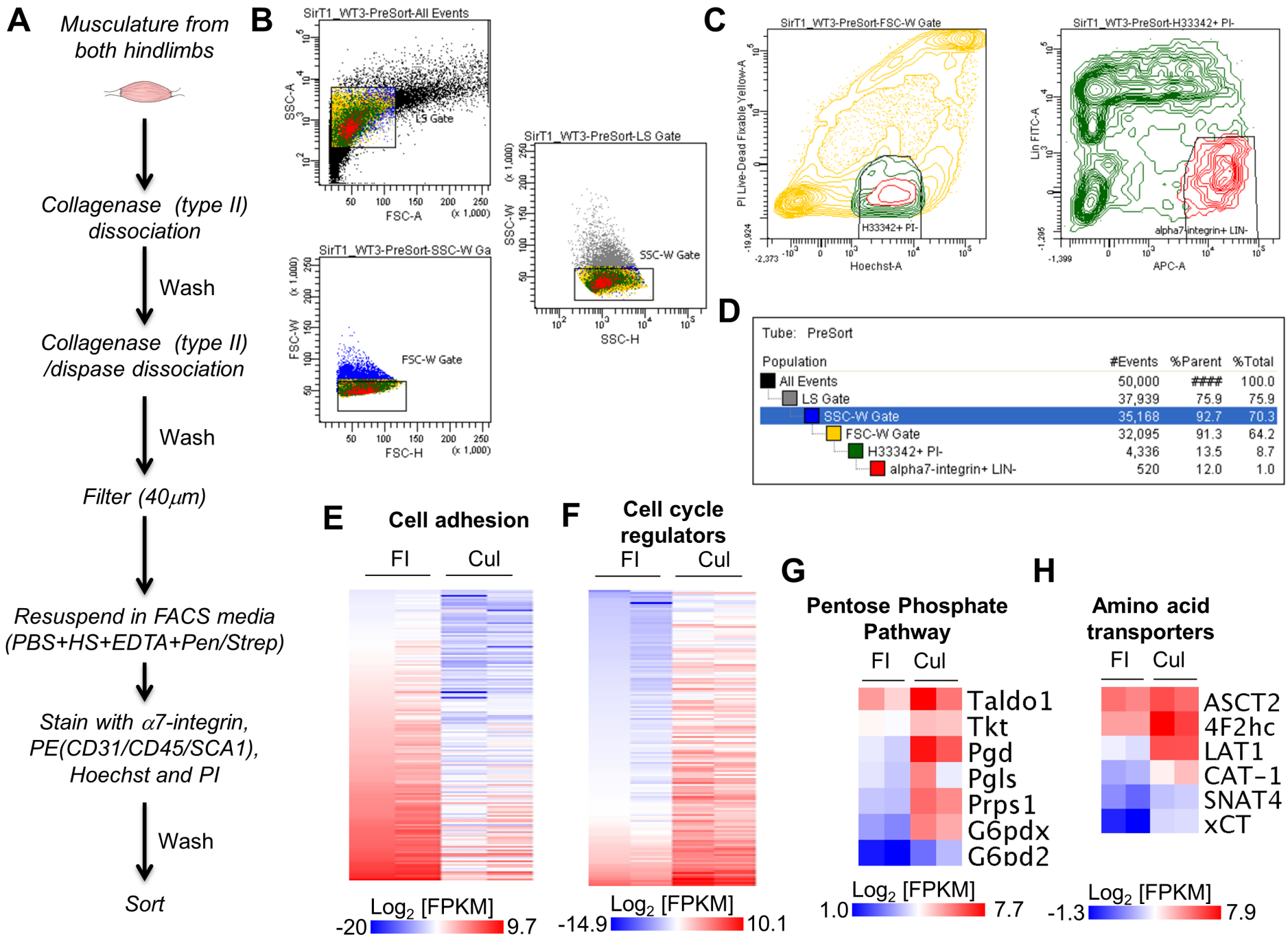

Ryall et al. 2014 FIG S1

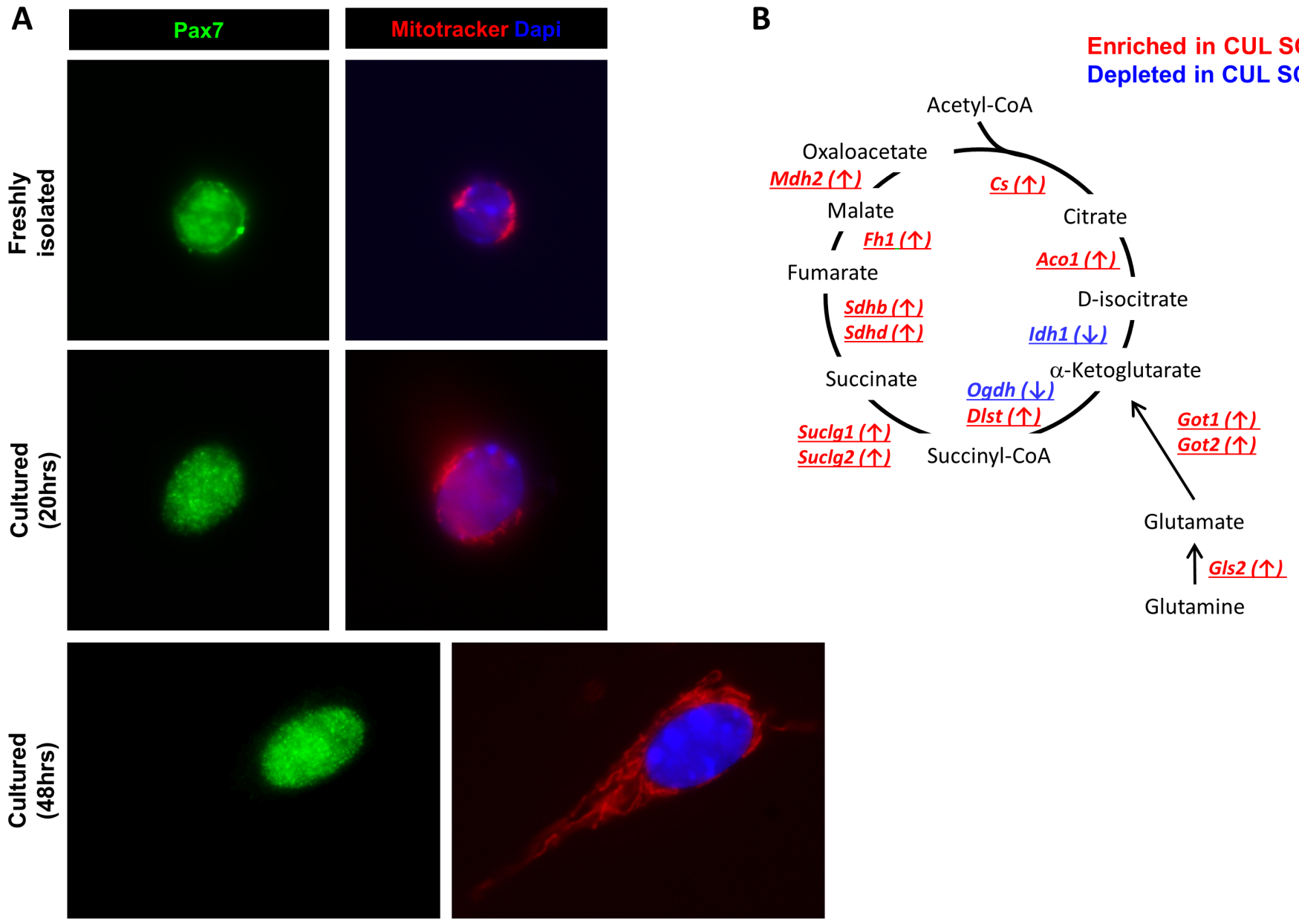

Ryall et al. 2014 FIG S2

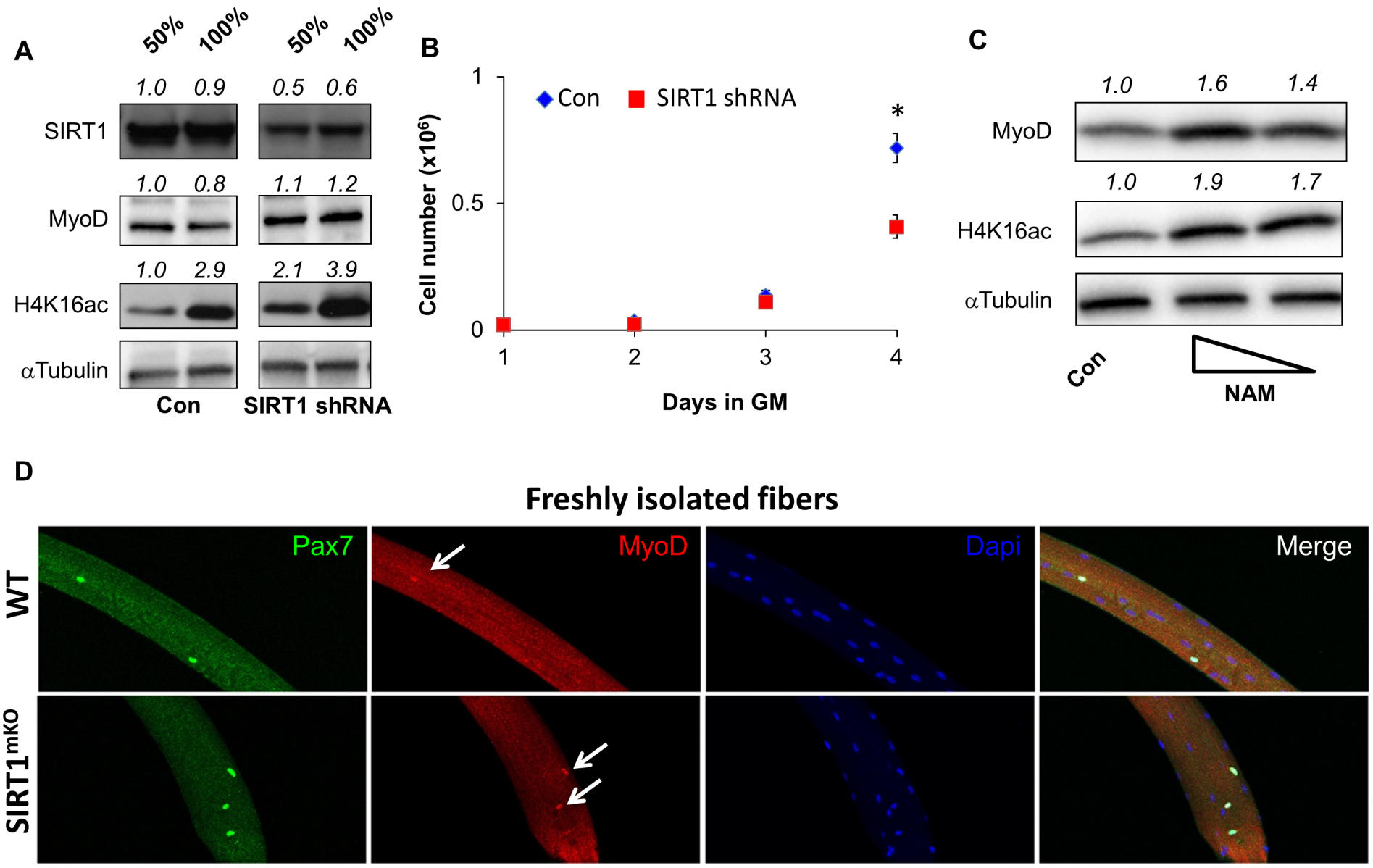

Ryall et al. 2014 FIG S3

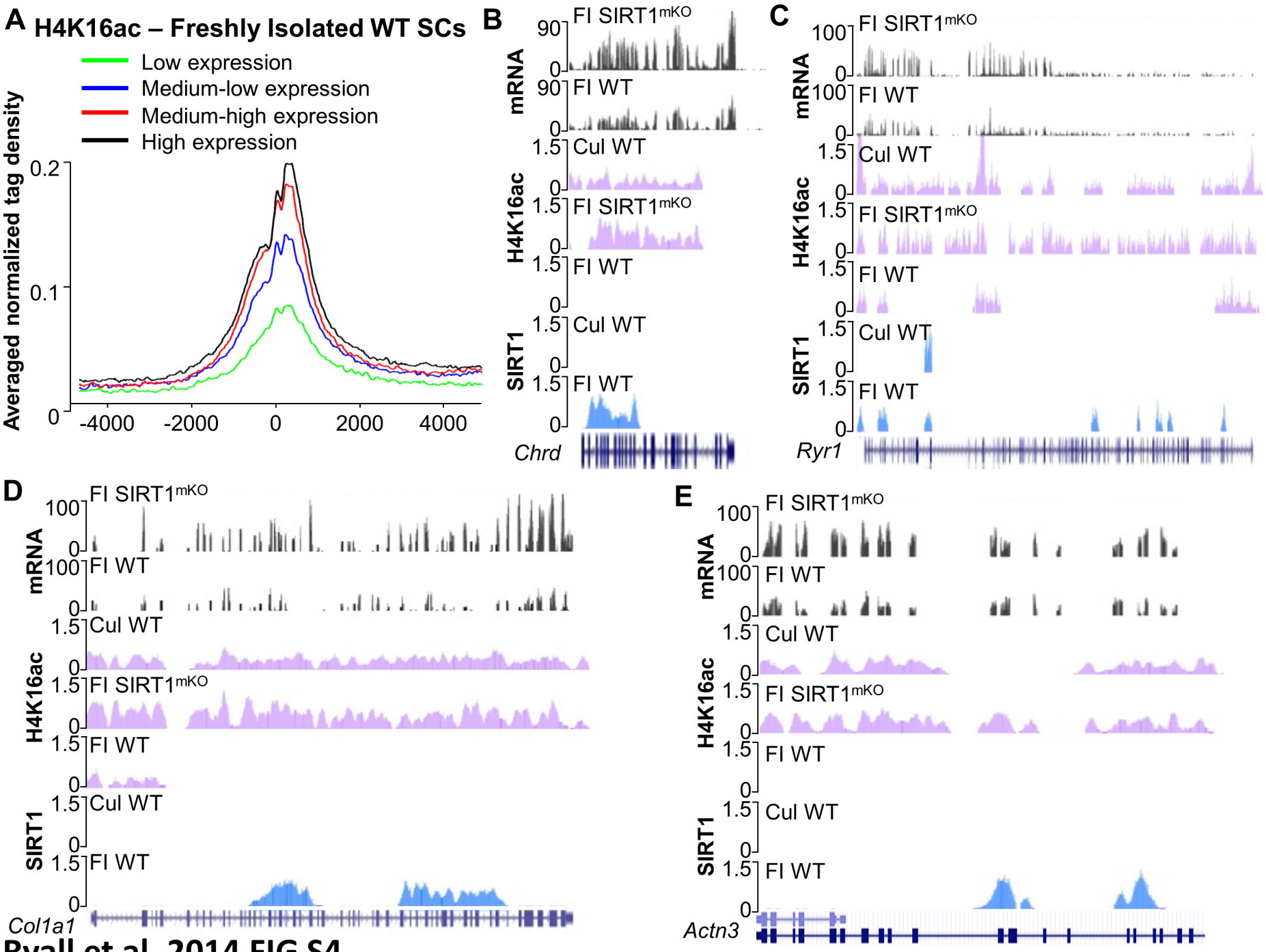

Ryall et al. 2014 FIG S4

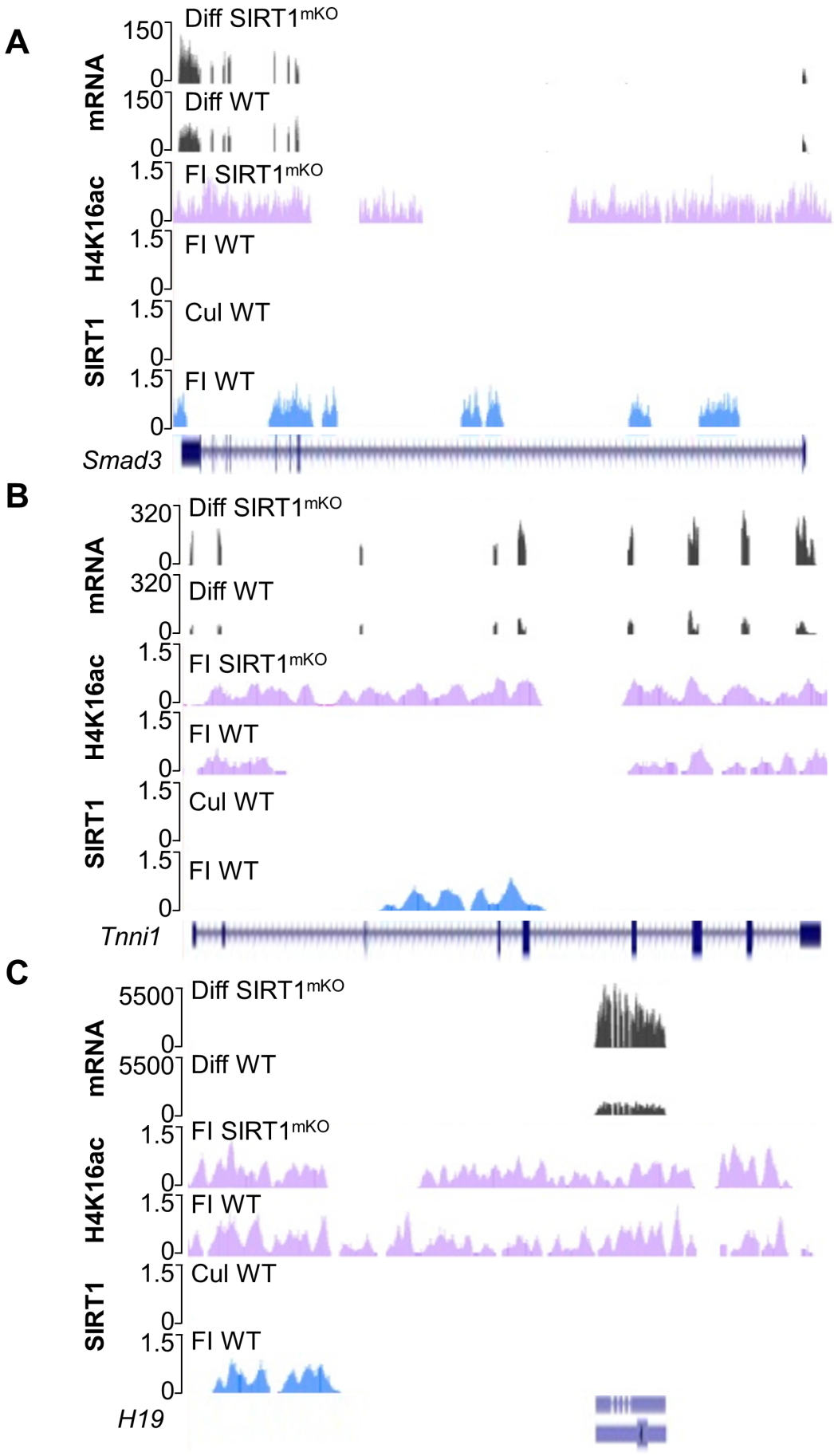

Ryall et al. 2014 FIG S5

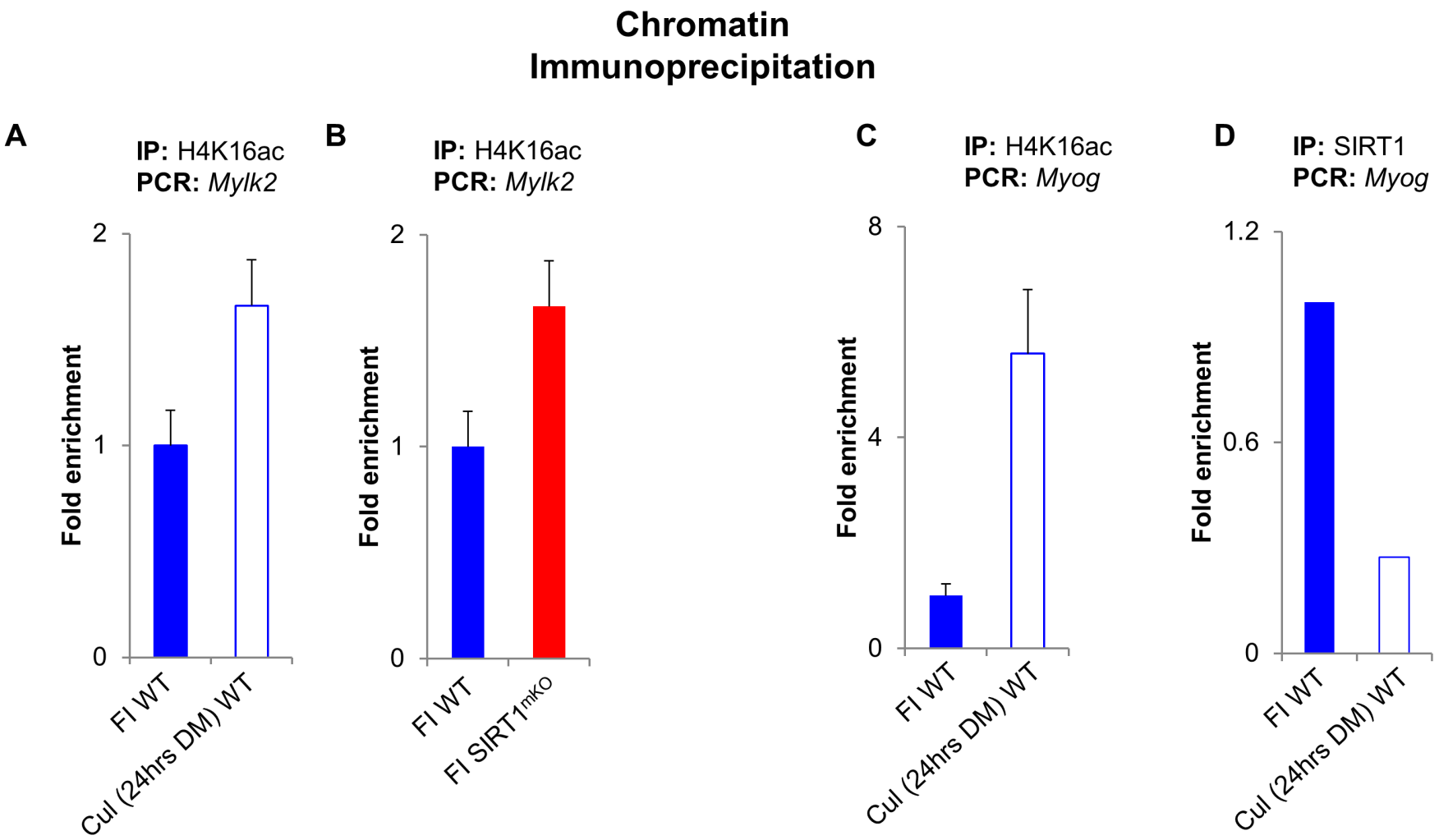

Ryall et al. 2014 FIG S6

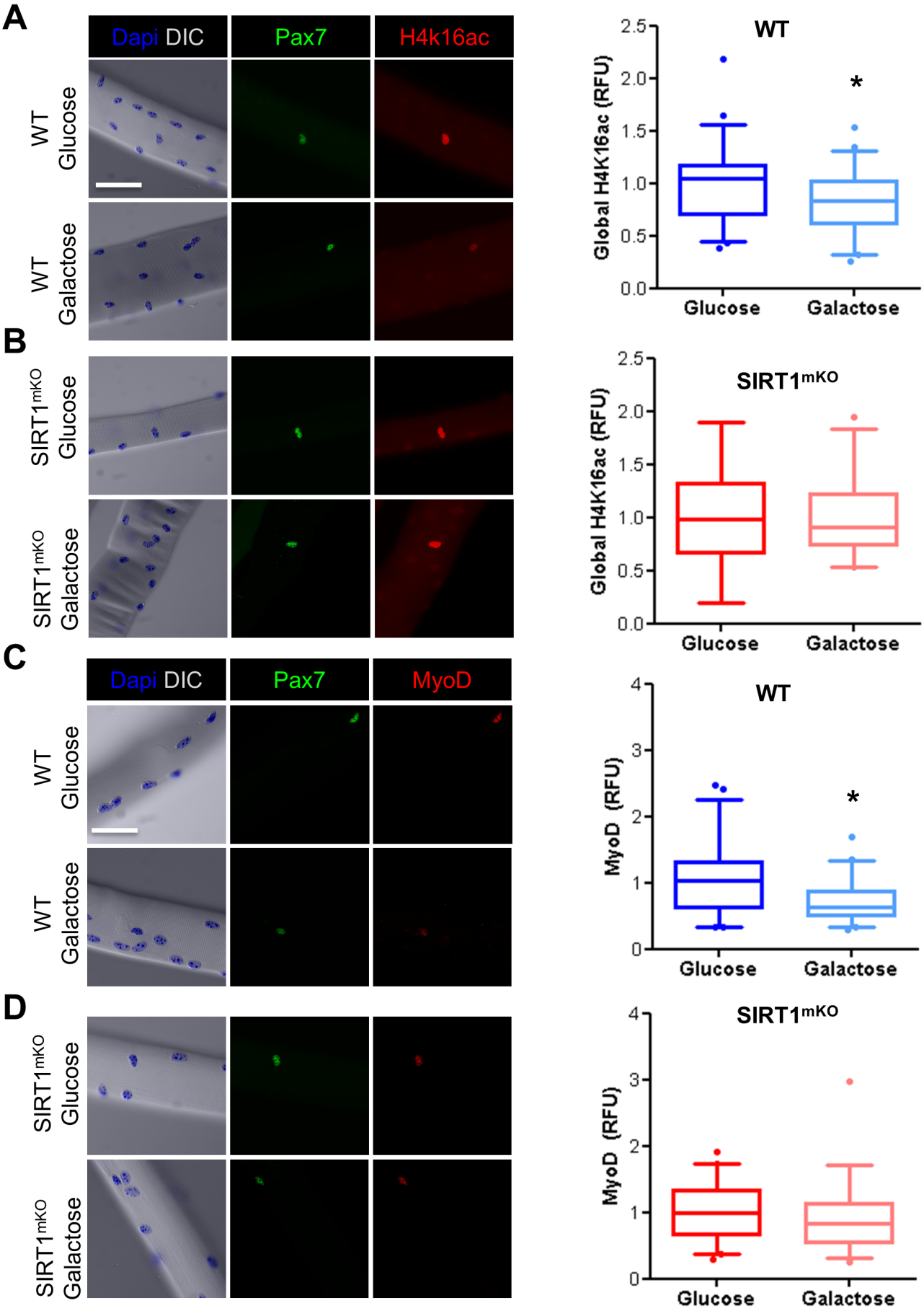

Ryall et al. 2013 FIGS7

SUPPLEMENTAL FIGURE LEGENDS

Figure S1, Related to Figure 1. FACS Isolated SCs Cultured in Growth Media Upregulate Cell-Cycle Genes, and Regulators of Biosynthesis

(A) Collagenase dissociation and staining protocol used for the FACS isolation of SCs (see Supplemental Experimental Procedures for additional details). (B-D) Representative FACS scatter plots indicating the population of cells classified as SCs. (E,F) Whole transcriptome analyses of SCs identified a significant enrichment of genes associated with cell adhesion in FI SCs (E), and cell-cycle progression in Cul SCs (F). (G,H) A targeted analysis of genes that regulate entry into pentose phosphate pathway (PPP) in Cul SCs (G). Similarly, these cells exhibited an enrichment of several genes encoding amino-acid transporters (H).

Figure S2, Related to Figure 1. Cultured SCs Undergo Mitochondrial Biogenesis but Exhibit an Abbreviated TCA Cycle

(A) MitoTracker staining of FI and Cul SCs (20 and 48hrs) cultured in growth conditions. (B) Genes that encode enzymes regulating progression through the TCA cycle were enriched in Cul SCs, with the exception of *Idh1* suggesting a reliance on glutaminolysis for the generation of α-ketoglutarate.

Figure S3, Related to Figures 3 and 4. Reduced Levels of SIRT1 Protein or Activity Leads to Increased MyoD and Global H4K16ac Levels in C2C12 Cells

(A) C2C12 cells were transduced with a control or SIRT1 shRNA retrovirus and their extracts immunoblotted with antibodies against SIRT1, MyoD, H4K16ac, and tubulin. 50% and 100% cell confluency. (B) Cell proliferation was evaluated in control and SIRT1 shRNA-transduced C2C12 cells. (C) C2C12 cells were treated with increasing concentrations of the SIRT1 inhibitor NAM and their extracts immunoblotted with antibodies against MyoD, H4K16ac, and tubulin. (D) Immunofluorescent analysis of single fibers from WT and $SIRT1^{mKO}$ mice stained with Pax7 and MyoD antibodies Dapi identies nuclei.

Figure S4, Related to Figure 6. Loss of SIRT1 Deacetylase Activity Leads to Altered H4K16 Acetylation and Expression of Selected Genes

(A) Average signal of normalized tag density for H4K16ac ChIP-seq in Freshly Isolated WT SCs for genes with low expression (green line), medium-low expression (blue line), medium high (red line) and high expression (black line) linking enrichment of H4K16ac to gene expression in SCs. (B) ChIP-seq and RNA-seq profiles of the *Chrd* gene. Bottom to top:

SIRT1 ChIP-seq profile in FI and Cul WT SCs (blue signals); H4K16ac profile in FI WT and SIRT11^{mKO} SCs, and WT Cultured SCs (magenta signals); *Chrd* mRNA expression profile in FI WT and SIRT1^{mKO} SCs (black signals). (C) ChIP-seq and RNA-seq profiles of the *Ryr1* gene. Bottom to top: SIRT1 ChIP-seq profile in FI and Cul WT SCs (blue signals); H4K16ac profile in FI WT and SIRT11^{mKO} SCs, and WT Cultured SCs (magenta signals); *Ryr1* mRNA expression profile in FI WT and SIRT1^{mKO} SCs (black signals). (D) ChIP-seq and RNA-seq profiles of the *Col1a1* gene. Bottom to top: SIRT1 ChIP-seq profile in FI and Cul WT SCs (blue signals); H4K16ac profile in FI WT and SIRT11^{mKO} SCs, and WT Cultured SCs (magenta signals); *Col1a1* mRNA expression profile in FI WT and SIRT1^{mKO} SCs (black signals). (E) ChIP-seq and RNA-seq profiles of the *Actn3* gene. Bottom to top: SIRT1 ChIP-seq profile in FI and Cul WT SCs (blue signals); H4K16ac profile in FI WT and SIRT11^{mKO} SCs, and WT Cultured SCs (magenta signals); *Actn3* mRNA expression profile in FI WT and SIRT1^{mKO} SCs (black signals).

Figure S5, Related to Figure 5 and 6. RNA-seq and ChIP-seq traces for Smad3, Tnni1, and H19 Loci.

(A) ChIP-seq and RNA-seq profiles of the *Smad3* gene. Bottom to top: SIRT1 ChIP-seq profile in FI and Cul WT SCs (blue signals); H4K16ac profile in FI WT and SIRT11^{mKO} SCs (magenta signals); *Smad3* mRNA expression profile in WT and SIRT1^{mKO} SCs induced to differentiate (black signals). (B) ChIP-seq and RNA-seq profiles of the *Tnni1* gene. Bottom to top: SIRT1 ChIP-seq profile in FI and Cul WT SCs (blue signals); H4K16ac profile in FI WT and SIRT11^{mKO} SCs (magenta signals); *Tnni1* mRNA expression profile in WT and SIRT1^{mKO} SCs induced to differentiate (black signals). (C) ChIP-seq and RNA-seq profiles of the *H19* gene. Bottom to top: SIRT1 ChIP-seq profile in FI and Cul WT SCs (blue signals); H4K16ac profile in FI WT and SIRT11^{mKO} SCs (magenta signals); *H19* mRNA expression profile in WT and SIRT1^{mKO} SCs induced to differentiate (black signals).

Figure S6, Related to Figure 6. H4K16ac is Enriched at Gene Loci of Cultured WT SCs and Freshly Isolated SIRT1^{mKO} SCs

(A,B) Chromatin immunoprecipitation with a H4K16ac antibody (n=2) followed by qPCR at the *Mylk2* locus demonstrated an enrichment of H4K16ac at the promoter region of (A) Cul (24hrs DM) WT SCs and (B) FI SIRT1^{mKO} SCs, compared to FI WT SCs. (C,D) Chromatin immunoprecipitation with a H4K16ac (n=2) (C) or SIRT1 (n=1) antibodies followed by

qPCR at the *Myog* locus demonstrated an enrichment of H4K16ac and a concomitant depletion of SIRT1 at the promoter region of Cul (24hrs DM) WT SCs.

Figure S7, Related to Figure 7. Satellite Cells from WT, but not SIRT1 ^{mKO} Mice, Exhibit Reduced Global H4K16ac and MyoD Expression when Forced to Utilize OXPHOS to Generate ATP

(A,B) Incubation in growth media containing galactose instead of glucose resulted in a decrease in global SC H4K16ac in WT (A), but not SIRT1^{mKO} (B) mice. (C-D) Incubation in growth media containing galactose instead of glucose resulted in a decrease in MyoD protein levels SCs from WT (C), but not SIRT1^{mKO} (D). Results were determined via relative fluorescence (RFU) in SCs labelled for H4K16ac or MyoD (n=3, >50 fibers/timepoint). White scale bar indicates 50μm. Results are presented as box-and-whisker plots, with a significant difference indicated when the median ± 95% CI does not overlap.

SUPPLEMENTAL TABLES

Table S1, Related to Figure 1. RNAseq FPKM, Fold-Change and Gene Ontology Results from Freshly Isolated and Cultured SCs

See separate excel File, Table S1.xlsx

Table S2, Related to Figure 5. RNAseq FPKM, Fold-Change and Gene Ontology Results from Freshly Isolated and Cultured SCs from WT and SIRT1^{mKO} Mice

See separate excel File, Table S2.xlsx

Table S3, Related to Figure 6. ChIPseq and Gene Ontology Results for H4K16ac Immunoprecipitated from Freshly Isolated and Cultured SCs from WT and SIRT1^{mKO} Mice

See separate excel File, Table S3.xlsx

Table S4, Related to Figure 6. ChIPseq Coordinates for SIRT1 from Freshly Isolated and Cultured SCs

See separate excel File, Table S4.xlsx

Table S5, Related to Figure 7. Microarray and Gene Ontology Results for RNA Isolated from the Gastrocnemius Muscles of Adult WT and SIRT1^{mKO} Mice

See separate excel File, Table S5.xlsx

SUPPLEMENTAL EXPERIMENTAL PROCEDURES

Antibodies

Acetyl Histone H4 (lys16), Sirt1(Sir2) (Millipore, Billerica, MA, USA); MyoD(C20) (Santa Cruz Biotechnology, Dallas, TX, USA); GAPDH (Abcam, Cambridge, MA, USA); αTubulin, Pax7 (Developmental Studies Hybridoma Bank, Iowa City, IA, USA).

PCR primers

Myog (ChIP) – (s) GAA TCA CAT GTA ATC CAC TGG AAA, (as) ACC CAG AGA TAA ATA TAG CCA ACG; *Mylk2* (ChIP) – (s) CTT AGT CTC CGC CTC CAC TG, (as) AGG CCA GTC AAC TGA GAG G; *Pax7* (qPCR) – (s) TCT CCA AGA TTC TGT GCC GAT, (as) CGG GGT TCT CTC TCT TAT ACT CC.

Metabolites

NAD^+, NADH and ATP were determined using commercially available kits (Biovision, Milpitas, CA), as per providers' instructions.

Transcriptome Sequencing and Bioinformatics

RNA-seq of FACS isolated SCs from WT and $SIRT1^{mKO}$ mice was completed on either an Illumina GAIIx or HiSeq2000 instrument, using cDNA libraries generated from poly A+ purified mRNA samples according to the manufacturer's instructions. Data from at least two independent runs of 36 and 50bp single-end reads were mapped to mouse genome (mm9 assembly) using TopHat (Trapnell et al., 2009), and gene transcript levels were determined via Cuffdiff in the form of FPKM (RPKM) values by correcting for multi reads and using geometric normalization (Trapnell et al., 2013). GO analyses of molecular function were analyzed using the online bioinformatics resource DAVID (National Institute of Allergy and Infectious Diseases, NIH) (Huang da et al., 2009a, b) and Metacore (Thomson Reuters).

Affymetrix Microarray

Total RNA was extracted from the gastrocnemius hindlimb muscles of WT and $SIRT1^{mKO}$ mice (n=3 samples/group). Samples were hybridized to an Affymetrix murine genechip as previously described (Fulco et al., 2008). Data were analyzed from three samples per group

with a greater than 1.5 fold change in gene expression and $p<0.05$ considered statistically different.

Analysis of ChIP Sequencing

ChIP-Seq data were obtained using an Illumina HiSeq 2000, with samples de-multiplexed via the Illumina pipeline, and mapped to the mouse genome (UCSC genome browser, mm9 version) using the Bowtie algorithm (Langmead et al., 2009). ChIP-Seq data generated from mock DNA immunoprecipitates (input DNA) were used against the sample data in calling enriched regions and to control for the false-positive detection rate (FDR). Enriched regions for H4K14ac were detected using the SICER algorithm at an FDR level of 5% with a window and gap size set to 200bp and 600bp, respectively (Zang et al., 2009). SIRT1 peaks were called using MACS version 1.4.1 (Zhang et al., 2008), with p-value set to 10^{-5} for enrichment against the input genomic DNA, background reads were shuffled and randomly down-sampled to adjust for the difference in read coverage between samples. Downstream analyses to generate intensity profile around the transcriptional start site (TSS), and correlative analysis with RNA-Seq data were completed using custom written codes in MATLAB.

Integrated Optical Density and Calculation of Relative Fluorescence Units

To analyze global H4K16ac and expression of MyoD protein levels in SCs attached to single fibers in a semi-quantitative manner we determined the integrated optical density (IOD) of SCs following indirect immunofluorescence. Following immunofluorescent labelling with an appropriate primary and secondary antibody, fluorescent images were captured under identical conditions on an upright microscope. Using ImageJ software (Schneider et al., 2012) the background fluorescence density was measured from a cytoplasmic region of the myofiber, and then the IOD (defined as the fluorescence intensity multiplied by the region of interest) was calculated for each $Pax7^{+}$ cell (SC) attached to that fiber. The final value of relative fluorescence units (RFU) was determined for each SC using the following calculation:

IOD (protein of interest) – (area of SC X background staining intensity)

Cellular Bioenergetics

Cellular bioenergetics were analysed on a Seahorse extracellular flux bioanalyzer (XF96) according to the manufacturer's instructions. Briefly, cells (FACS isolated SCs or C2C12

cells) were seeded at a density of $50x10^3$ cells/well (SCs) or $12x10^3$ cells/well (C2C12 cells) in a Seahorse XF96 plate. The seeding density was based upon an initial assay that optimised OCR and ECAR, and minimised variability. Cells were cultured overnight in growth media. Immediately prior to the assay, cultured cells were washed twice in minimal assay media (Seahorse Biosciences, 37°C, pH 7.40) supplemented with 25mM glucose and 1mM sodium pyruvate. All cells were equilibrated in minimal assay media for 45-60mins in a non-CO_2 incubator immediately prior to the assay. The basal rate of oxygen consumption (OCR) and extracellular-acidification rate (ECAR) were measured in triplicate for 2mins (over a total of 15mins) from the rate of decline in O2 partial pressure (OCR), and rate of change in assay pH (ECAR).

Cell Culture Media

C2C12 cells were grown in DMEM supplemented with 20% FBS, and differentiated at confluence in DMEM supplemented with 2% HS (see below for details). A stable C2C12 SIRT1 shRNA line was generated via standard transfection techniques as described previously (Fulco et al., 2008).

SC growth media: Hams F-10 media (Gibco), 20% fetal bovine serum (FBS, Gibco), bFGF (12.5ng/mL), Penicillin/streptomycin (1x, Gibco).

C2C12 growth media: DMEM (no glucose, no sodium-pyruvate, Gibco), 25mM Glucose (Sigma-aldrich) or 10mM Galactose (Sigma-aldrich), 20% FBS (Gibco), Penicillin/streptomycin (1x, Gibco).

C2C12 differentiation media: DMEM (25mM glucose, no sodium-pyruvate, Gibco), 2% horse serum (Gibco), Penicillin/streptomycin (1x, Gibco).

Single fiber growth media: DMEM (25mM glucose, 1mM sodium-pyruvate, Gibco), 10% heat-inactivated horse serum (Gibco), 0.5% chick embryo extract (US Biologicals), Penicillin/streptomycin (1x, Gibco).

SUPPLEMENTAL REFERENCES

Fulco, M., Cen, Y., Zhao, P., Hoffman, E.P., McBurney, M.W., Sauve, A.A., and Sartorelli, V. (2008). Glucose restriction inhibits skeletal myoblast differentiation by

activating SIRT1 through AMPK-mediated regulation of Nampt. Dev. Cell *14*, 661-673.

Huang da, W., Sherman, B.T., and Lempicki, R.A. (2009a). Bioinformatics enrichment tools: paths toward the comprehensive functional analysis of large gene lists. Nucleic Acids Res *37*, 1-13.

Huang da, W., Sherman, B.T., and Lempicki, R.A. (2009b). Systematic and integrative analysis of large gene lists using DAVID bioinformatics resources. Nat Protoc *4*, 44-57.

Langmead, B., Trapnell, C., Pop, M., and Salzberg, S.L. (2009). Ultrafast and memory-efficient alignment of short DNA sequences to the human genome. Genome Biol *10*, R25.

Schneider, C.A., Rasband, W.S., and Eliceiri, K.W. (2012). NIH Image to ImageJ: 25 years of image analysis. Nat Methods *9*, 671-675.

Trapnell, C., Hendrickson, D.G., Sauvageau, M., Goff, L., Rinn, J.L., and Pachter, L. (2013). Differential analysis of gene regulation at transcript resolution with RNA-seq. Nature Biotechnology *31*, 46-53.

Trapnell, C., Pachter, L., and Salzberg, S.L. (2009). TopHat: discovering splice junctions with RNA-Seq. Bioinformatics *25*, 1105-1111.

Zang, C., Schones, D.E., Zeng, C., Cui, K., Zhao, K., and Peng, W. (2009). A clustering approach for identification of enriched domains from histone modification ChIP-Seq data. Bioinformatics *25*, 1952-1958.